

Supplementary Information

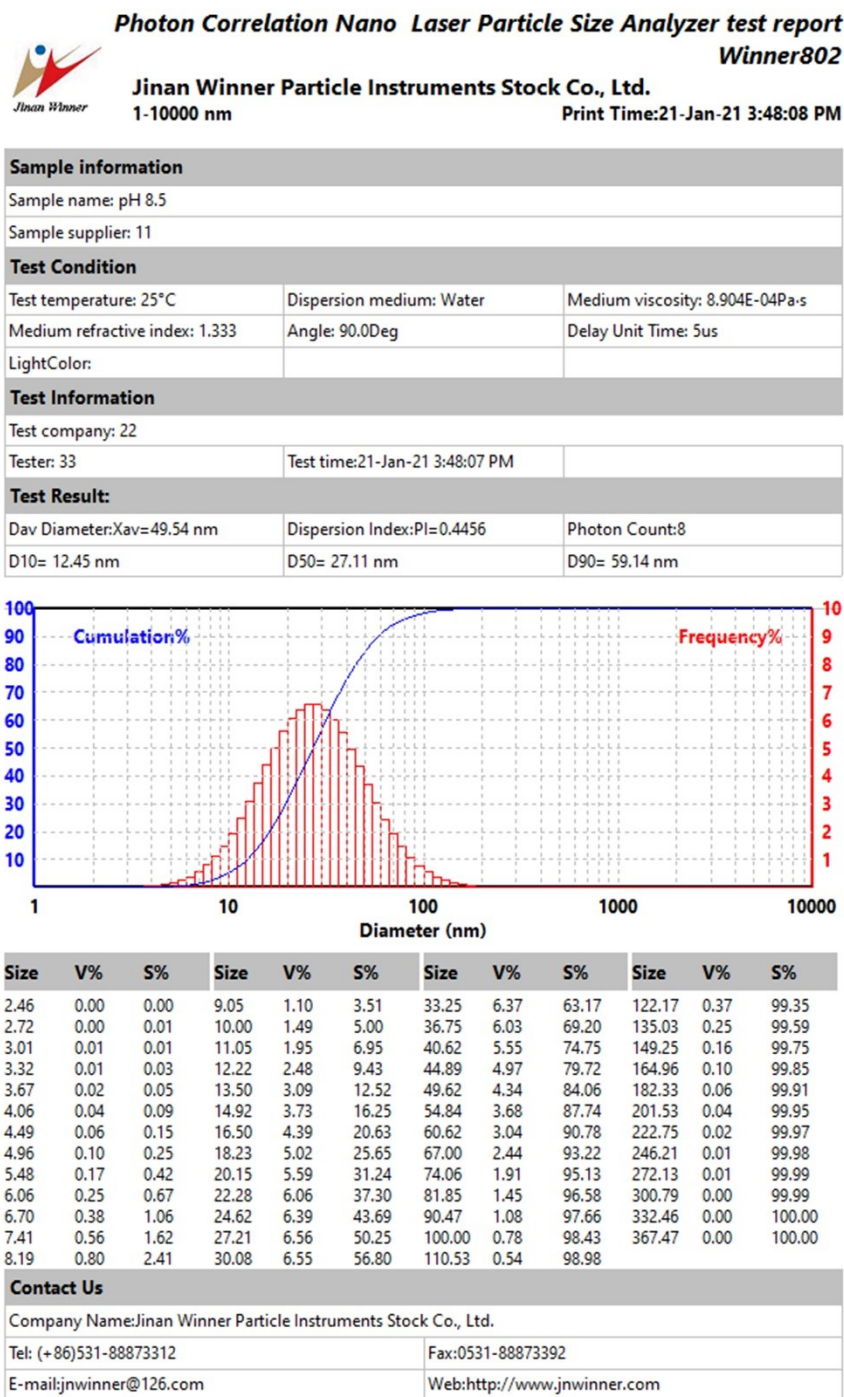


Figure S1. A DLS result of the guava leaf extract-synthesized AgNPs.

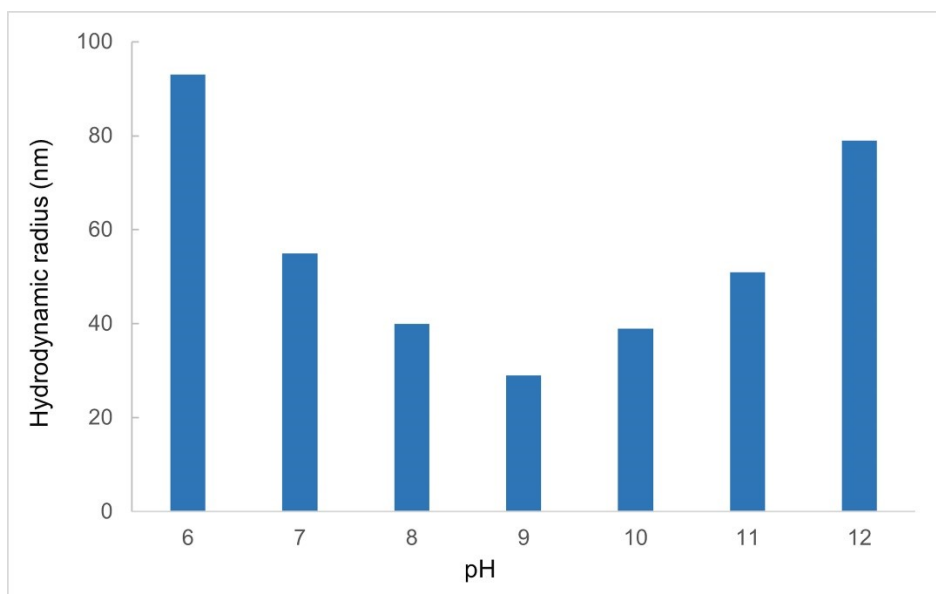


Figure S2. Hydrodynamic radius of AgNPs-GuLE synthesized at different pH conditions.

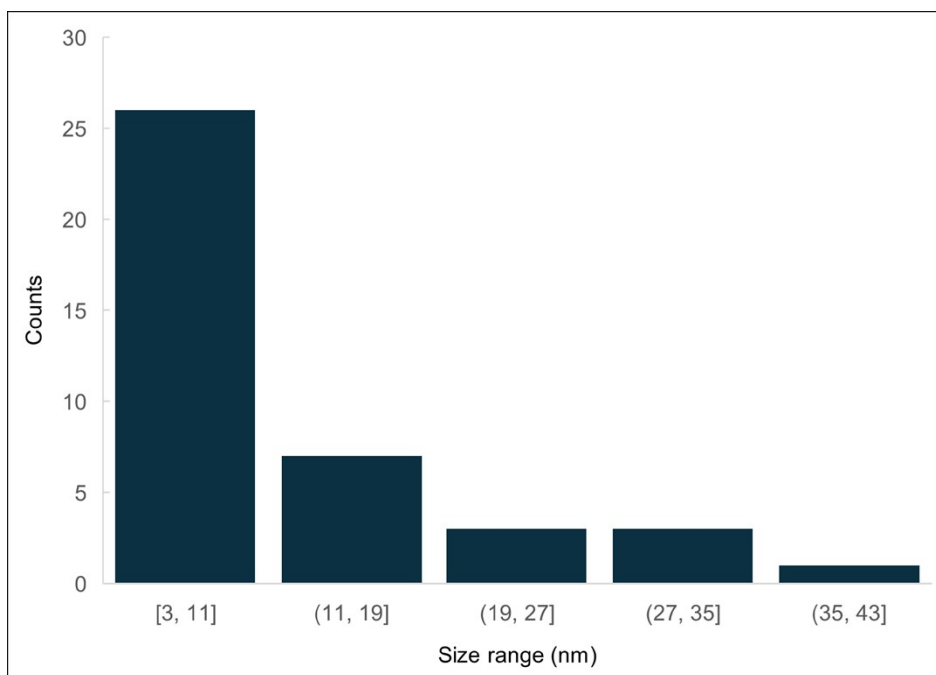


Figure S3. Histogram of AgNPs-GuLE's size distribution based on the TEM image.

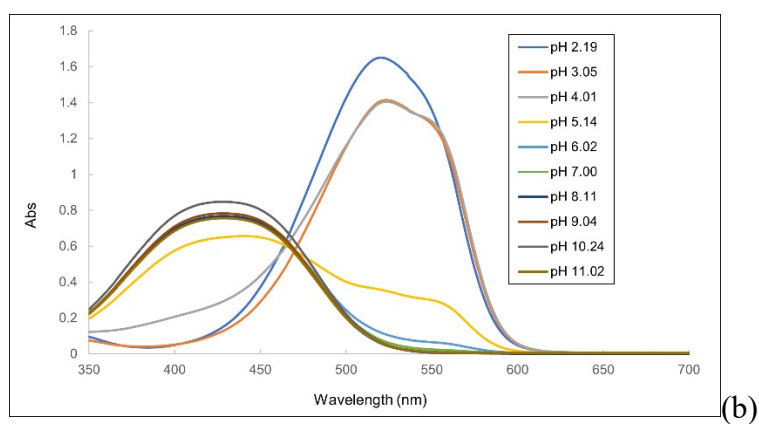
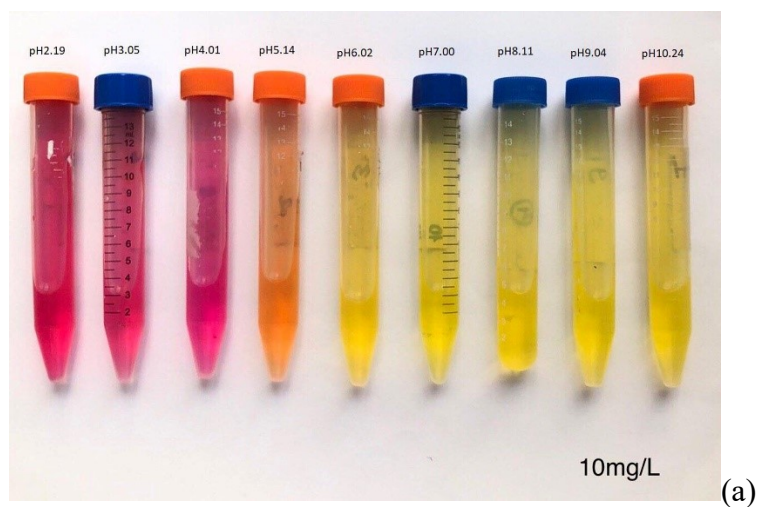
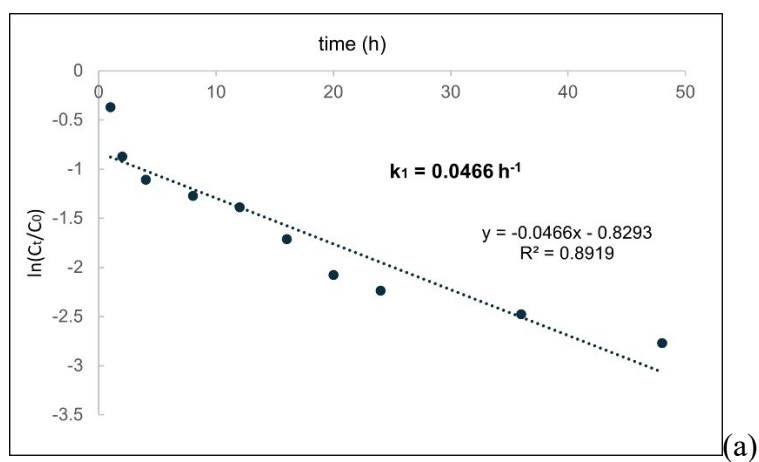


Figure S4. The color change of MR at varying pH (a) and the corresponding UV-Vis spectra (b).



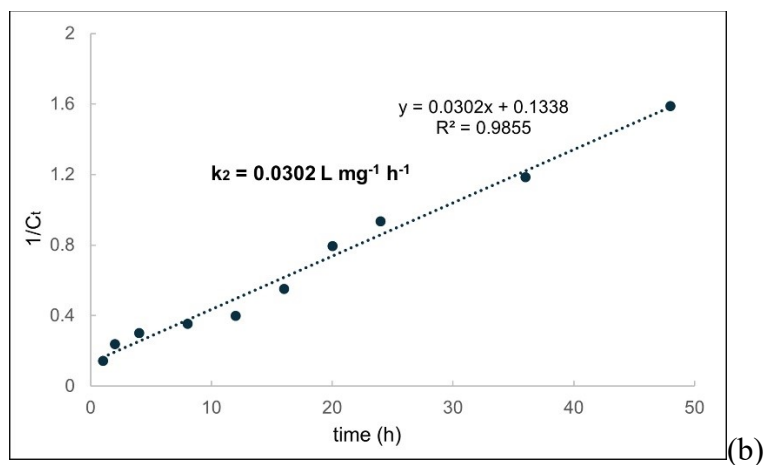


Figure S5. Plots of the pseudo-first-order kinetic (PFO) model [$\ln(C_t/C_0) = -k_1t$] (a) and the pseudo-second-order (PSO) kinetic model [$1/C_t - 1/C_0 = k_2t$] (b) (C_t is the MR's concentration at any light exposure time, C_0 represents the initial MR's concentration, k_1 denotes the PFO rate constant, and k_2 is designated as the PSO rate constant).

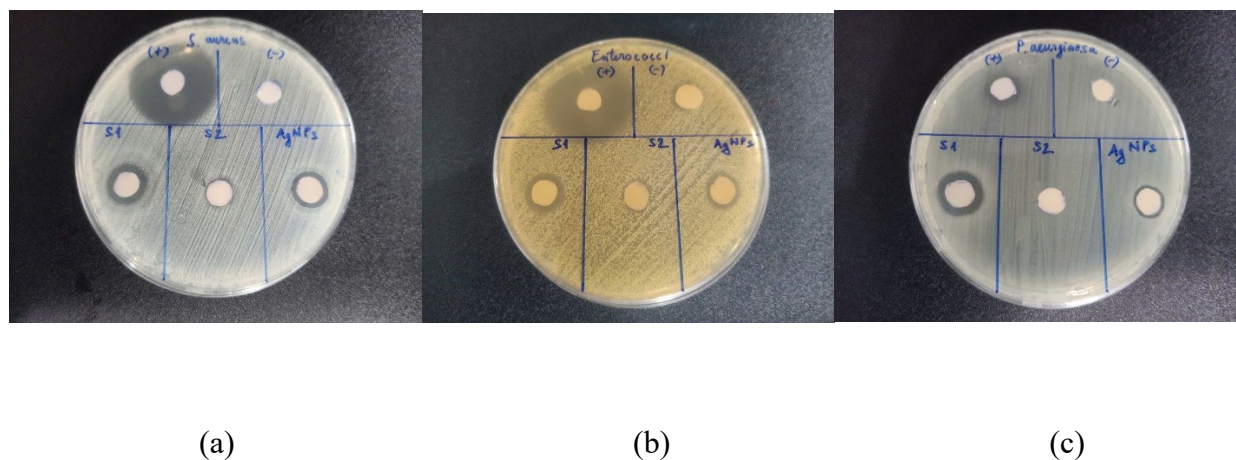


Figure S6. Results of antibacterial activity of AgNO_3 (S1), guava leaf extract (S2), and guava leaf extract-synthesized AgNPs against *S. aureus* (a), *E. faecalis* (b), and *P. aeruginosa* (c). (negative control: distilled water; positive control: chloramphenicol 30 mg/L).

Table S1. Preliminary assessment of the AgNPs-GuLE's reusability in the MR photocatalytic degradation.

Cycle	%PD (\pm SD)
1	$96 \pm 0.2 \%$
2	$71.6 \pm 2.4 \%$
3	$76.1 \pm 3.2 \%$